

# Neutrino Flavor Transformations from New Short-Range Forces

B.J.P. Jones

*University of Texas at Arlington, 108 Science Hall, 502 Yates St, Arlington TX, 76019*

J. Spitz

*University of Michigan, 450 Church St, Ann Arbor MI 48109*

(Dated: September 23, 2021)

We examine the commonly explored beyond-standard-model physics scenario of secret neutrino forces, and point out a model prediction that appears to have been overlooked: the generation of unique flavor-changing effects in experiments featuring decay-at-rest (DAR) neutrino sources. These flavor changes occur because the decay that drives neutrino and antineutrino production,  $\mu^+ \rightarrow e^+ + \bar{\nu}_\mu + \nu_e$ , is unique in producing two neutrinos in the final state. Any non-flavor-universal force between the emerging neutrinos would thus induce a new oscillation phase as they escape from each-other's potential wells, an effect which is largely absent in experiments that primarily rely on meson decay-in-flight and nuclear decay. We calculate the magnitude of the associated observable and compare it to the anomalous neutrino flavor transformation seen by the LSND experiment, finding a wide but constrained allowed parameter space. We also evaluate existing limits from other experiments, and the testability of this new effect at the future DAR programs JSNS<sup>2</sup> and OscSNS.

## INTRODUCTION

The LSND experiment [1] observed a  $3.8\sigma$  excess of  $\bar{\nu}_e$ -like interactions above the background from a  $\pi^+/\mu^+$  decay-at-rest (DAR) neutrino source at a distance of 30 m. The excess of  $87.9 \pm 22.4^{\text{stat}} \pm 6.0^{\text{syst}}$  events [2] can be interpreted in terms of short-baseline neutrino oscillations caused by one or more sterile flavors [3], with an oscillation probability between the source and detector of around 0.26%.

DAR neutrino experiments, like LSND, take advantage of both a precisely known neutrino ( $\nu_\mu$ ,  $\nu_e$ ,  $\bar{\nu}_\mu$ ) energy spectrum and interaction cross section from 0-52.8 MeV, and contain minimal contamination ( $\sim 10^{-3}$ ) from intrinsic  $\bar{\nu}_e$  [4]. A DAR source utilizes protons impinging on a target to produce charged pions  $\pi^\pm$ , which quickly come to rest there or in the surrounding shielding to produce neutrinos through the chain:

$$\pi^+ \rightarrow \mu^+ + \nu_\mu \quad (1)$$

$$\mu^+ \rightarrow e^+ + \nu_e + \bar{\nu}_\mu \quad (2)$$

Notably, no  $\bar{\nu}_e$  are present in Eqs. 1 and 2. Therefore, if a significant number of  $\bar{\nu}_e$ , detected via  $\bar{\nu}_e p \rightarrow e^+ n$ , are observed over backgrounds, a natural hypothesis is that the only available antineutrino  $\bar{\nu}_\mu$  must have oscillated to  $\bar{\nu}_e$ . The challenge for this explanation is that the baseline required to observe a significant number of events from the  $4\pi$  neutrino source, typically 10s of meters, is orders of magnitude too short to produce a discernible oscillation signature, given the known neutrino mass splittings [3]. Introducing additional neutrino mass states with a larger  $\Delta m^2$  and associated sterile flavors can produce effects at shorter baselines. But, severe tensions [5, 6] between the allowed regions from positive results like LSND and MiniBooNE [7] and the non-observation of anomalous oscillations in  $\nu_\mu$  and  $\bar{\nu}_\mu$  disappearance experiments [8, 9]

mandate the careful consideration of other explanations, both novel and mundane, for the LSND anomaly.

A beyond-standard-model scenario that has been considered in a variety of contexts invokes “secret” interactions [10] between new force carriers and neutrinos, absent for the other standard model particles (recent Refs. include [11–15]). For example, new forces between active neutrinos can arise in a gauge invariant fashion if the new mediator couples to right handed neutrinos directly, followed by mixing with active neutrinos after electroweak symmetry breaking. Here, we do not commit to any specific UV completion, but investigate a general consequence of classes of theories with secret neutrino forces for experiments using DAR sources such as LSND.

## FLAVOR CHANGE FROM NEW FORCES

DAR-based experiments are unique among oscillation probes in that each  $\mu^+$ -decay antineutrino is produced alongside a neutrino. Since these two particles emerge from the decay of a single muon, they are produced in close spatial proximity, separating as they leave the decay vertex. Given new forces between neutrinos, the emerging neutrino and antineutrino will experience a mutual potential as they separate. If the couplings of the neutrinos to the new field are not mass-universal, the process of escaping from this potential will imbue the neutrino/antineutrino produced in muon decay with an additional oscillation phase compared to those produced in, for example, charged-pion decay, where only one neutrino is emitted. In essence, the  $\mu^+$  will not simply decay to  $\bar{\nu}_\mu$  and  $\nu_e$ , but to slightly flavor-transmuted states. This transformation occurs within a very short distance of the decay vertex and is a generic consequence of new, non-universal forces between neutrinos, independent of

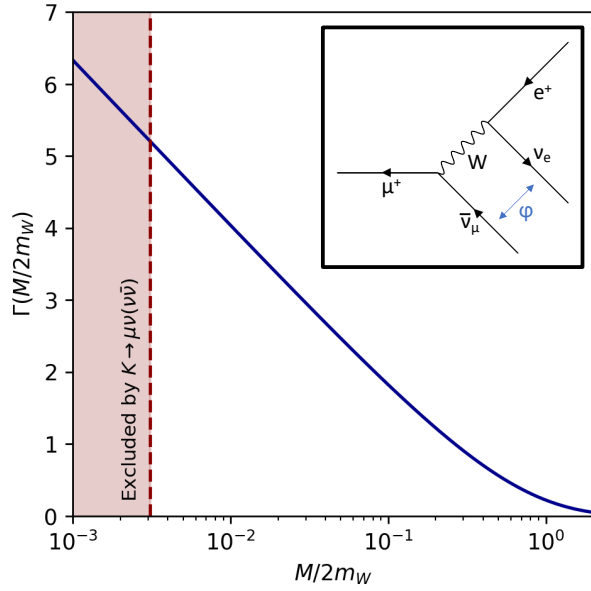


FIG. 1. The incomplete gamma function which dictates the scale of the phase shift induced by the new force. Inset: a Feynman diagram from muon decay with the new force indicated.

the detailed properties of the mediator, except coupling strength and mass.

Neutrino flavor oscillations are a consequence of phase differences between propagating neutrino mass states. This phase difference between states  $i$  and  $j$  can be expressed as  $\phi_{ij} = \int dt [E_i(t) - E_j(t)] / \hbar$ . Taylor expanding  $E_i = \sqrt{p^2 + m_i^2}$  in the limit of small  $m_i^2/p^2$  yields the standard neutrino oscillation phase:

$$\phi_{ij} = \int dt \frac{\Delta m_{ij}^2}{2p} \hbar \approx \frac{\Delta m_{ij}^2 L}{2E}. \quad (3)$$

The latter equality assumes highly relativistic neutrinos, so  $t \sim L$  and  $p \sim E$ , and adopts natural units  $\hbar = c = 1$ . Other non-flavor-universal contributions to the neutrino energy will also induce phase shifts—for example, in sufficiently high density environments neutrinos experience a matter potential due to the abundance of  $e^-$  in matter, as compared to  $\mu^-$  and  $\tau^-$  [16, 17]. The hypothetical role of a phase due to gravitational fields has also been explored [18, 19].

Considering models with new forces between neutrinos, one must also include contributions to the neutrino energy from mutual attraction or repulsion. The effective range  $r$  of a force carried by a mediator with mass  $M$  follows the Yukawa potential [20]:

$$V_{ab}(r) = \frac{g_a g_b}{4\pi} \frac{e^{-Mr}}{r}, \quad (4)$$

where  $g_a, g_b$  are the couplings to each particle. As discussed below, experimental bounds are strong for mediator masses below  $\sim 500$  MeV, so the relevant distance

scales must be short (1 fm or less). No two neutrinos produced in independent decays are thus expected to reach sufficient proximity to impact each other's oscillations in experimental conditions. For neutrinos produced in a common decay, however, there is at least momentary proximity where the force will be significant.

To find the contribution of this potential to oscillations, we integrate the quantum phase as the neutrinos escape from each other's potential wells. The total phase is Lorentz invariant, and we choose to perform the calculation in the reference frame where the recoiling  $\nu_e$  is at rest, so the  $\nu_e$  is considered as a source of the potential from which the  $\bar{\nu}_\mu$  escapes. Because the neutrinos are very light relative to the Q-value of the decay, we can safely assume that the  $\bar{\nu}_\mu$  moves at  $c$  in this frame at all times. The total phase shift of an antineutrino mass state  $i$  due to a recoiling neutrino mass state  $a$  is then:

$$\phi_{ia} = \int_0^\infty dt V(t) = g_i g_a \int_{r_0}^\infty dr \frac{e^{-Mr}}{r}. \quad (5)$$

We have assumed the couplings to be non-universal but diagonal in the mass basis for simplicity of exposition, though non-diagonal couplings can be accommodated with a trivial extension. In Eq. 5,  $r_0$  is the separation at which the  $\nu_e$  and  $\bar{\nu}_\mu$  are produced. This distance scale is determined by the range of the virtual  $W$  boson separating the two vertices in the Feynman diagram of Fig. 1. Order-of-magnitude estimates suggest the range of the weak force,  $r_0 \sim 1/m_W$ . A more nuanced calculation (Appendix 1) gives  $r_0 \sim 1/2m_W$  as the mean distance of the Yukawa interaction. Since our results depend only logarithmically on this scale, the precise pre-factor is somewhat unimportant.

The integral of Eq. 5 can be evaluated to yield:

$$\phi_{ia} = g_i g_a \Gamma\left(0, \frac{M}{2m_W}\right), \quad (6)$$

where  $\Gamma$  is the incomplete Gamma function, shown in Fig. 1. To calculate the neutrino transmutation probability we consider the entangled flavor-space wave functions of the recoiling  $\nu_e$  and  $\bar{\nu}_\mu$ . The initial state is:

$$|\psi(t_0)\rangle = |\nu_e\rangle \otimes |\bar{\nu}_\mu\rangle = \sum_{ia} U_{ea} U_{\mu i}^* |\nu_a\rangle \otimes |\bar{\nu}_i\rangle, \quad (7)$$

with  $U$  being the leptonic (PMNS) mixing matrix. Once the antineutrino has effectively escaped the potential generated by the neutrino in its rest frame, the flavor-space wave function is:

$$= \sum_{ia\alpha\beta} U_{ea} U_{\mu i}^* U_{\alpha a}^* U_{\beta i} \exp\left[ig_i g_a \Gamma\left(0, \frac{M}{2m_W}\right)\right] |\nu_\alpha\rangle \otimes |\bar{\nu}_\beta\rangle. \quad (8)$$

The flavor change probability for the antineutrino from

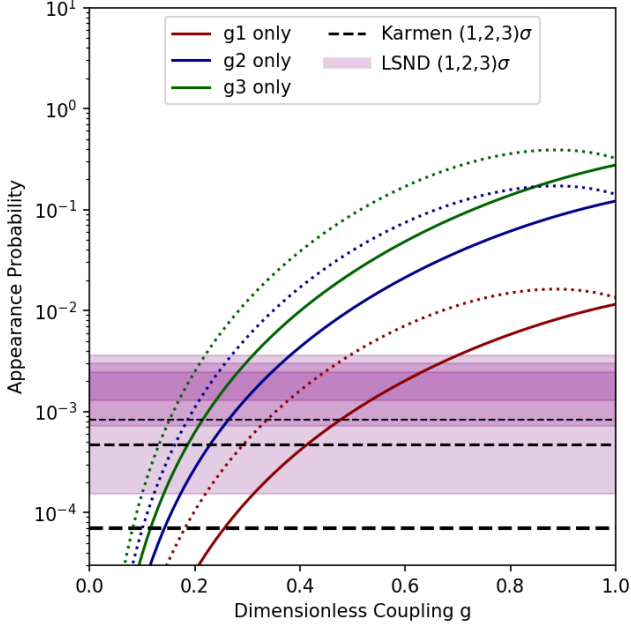


FIG. 2. Appearance probabilities given a single active coupling, with others set to zero for  $\Gamma = 2$  (solid lines) and  $\Gamma = 4$  (dotted lines).

$\bar{\nu}_\mu$  to  $\bar{\nu}_e$  is given by tracing out the unobserved neutrino:

$$P(\bar{\nu}_\mu \rightarrow \bar{\nu}_e) = \sum_\gamma |(\langle \nu_\gamma | \otimes \langle \bar{\nu}_e |) |\psi(t')\rangle|^2 \quad (9)$$

$$= \sum_\gamma \left| \sum_{ia} U_{ea} U_{\mu i}^* U_{\gamma a}^* U_{ei} \exp \left[ i g_i g_a \Gamma \left( 0, \frac{M}{2m_W} \right) \right] \right|^2 \quad (10)$$

Thus, given  $M$ ,  $g_1$ ,  $g_2$  and  $g_3$  and the PMNS matrix, we can calculate the transmutation probability.

As an initial exploration, we consider setting all the  $g$ 's to zero except for one, and examine the probability to transmute as a function of the remaining coupling. Under this scenario, and given the standard values of the PMNS elements with normal ordering [21], the appearance probabilities for single non-zero  $g$  are shown in Fig. 2. Also shown is the allowed region band of appearance probabilities consistent with the LSND excess at  $\pm 1, 2, 3\sigma$ , from Ref. [2]. Natural couplings within the perturbative regime at a scale of  $g \sim 0.1$  appear apt to explain the anomalous appearance rate at LSND. The observed energy spectrum is also consistent: Fig. 4 shows the LSND beam data overlaid on the expectation for energy-independent  $\bar{\nu}_\mu \rightarrow \bar{\nu}_e$  transmutations, normalized to the LSND excess and accounting for energy resolution [1]. A simple comparison, neglecting correlations, provides a  $\chi^2 = 7.8$  for 10 dof (prob.=0.65).

The KARMEN experiment [23] also used a DAR source at 17.7 m to search for short-baseline neutrino oscillations and observed 15  $\bar{\nu}_e$ -like events over a predicted background of  $15.8 \pm 0.5$ . This null result presents a constraint on nearly any beyond-standard-model inter-

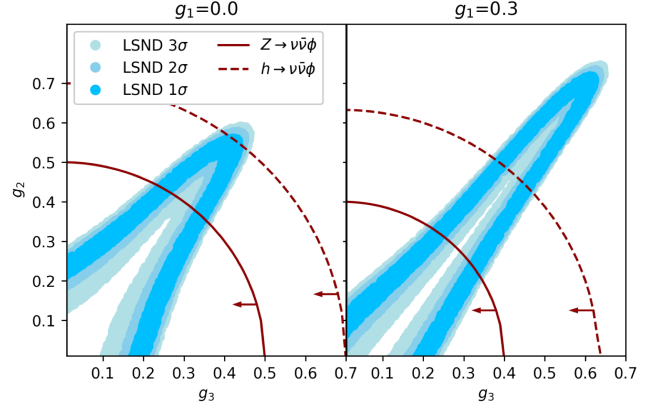


FIG. 3. LSND allowed regions given a 1 GeV mediator with all  $g$ 's nonzero. Each plot explores values of  $g_2$  and  $g_3$  given a fixed  $g_1$  and includes constraints on the invisible Higgs and  $Z$  boson widths from Ref. [22]

pretation of LSND, although the KARMEN measurement is statistically much weaker than the LSND observation. Assuming both measurements to have been performed correctly, we can compare them directly. To estimate the KARMEN constraint, we consider a counting experiment and construct 1, 2, and 3 $\sigma$  regions using the Feldman-Cousins approach [24]. The persistent tension between LSND and KARMEN visible in Fig. 2 represents a generic challenge for nearly all explanations of the LSND anomaly, and although the disagreement should not be overlooked, we do not consider it as especially detrimental for the viability of this new physics explanation relative to others.

For a more complete exploration of the parameter space, all three couplings must be allowed to be non-zero. Since  $g_2$  and  $g_3$  have the largest impact, we fix  $g_1$  at discrete values and make 2D contours in  $g_2, g_3$  space. For each point, we draw a random value of  $g_2$  and  $g_3$ , calculate the probability of flavor change, and test whether it lies within the allowed LSND region given 1, 2, and 3 $\sigma$  statistical fluctuations. A large and degenerate region of parameter space appears consistent with LSND (Fig 3).

While naturalness arguments might favor order-1 couplings for fundamental interactions, existing experimental limits must be accounted for where applicable. Constraints on secret neutrino interactions are collected in various works, including Refs. [10, 22]. Below the kaon mass, large neutrino-mediator coupling constants are forbidden due to the absence of unobserved processes such as  $K^+ \rightarrow (\nu\bar{\nu})\mu^+\nu$  [25]. These limits effectively rule out scenarios with experimentally observable consequences for  $M \leq m_K$ , shown as a vertical line in Fig. 1. For larger mediator masses, experimental constraints are much weaker. The strongest direct bound for  $M \geq 1$  GeV derives from the non-observation of the process  $Z \rightarrow \nu\bar{\nu}\phi$  via the invisible width of the  $Z$  [26]. This imposes a requirement that  $g < 0.5$  given a single-coupling-constant

Experiment	OscSNS	JSNS <sup>2</sup>
Runtime	5 calendar years	5 calendar years
Baseline	60 m	24 m
POT/year	$2.2 \times 10^{23}$	$3.8 \times 10^{22}$
Proton kinetic energy	1 GeV	3 GeV
$\mu^+$ (DAR) $\bar{\nu}_\mu$ /proton	0.12	0.30
Fiducial mass	450 ton	17 ton
$\bar{\nu}_e$ efficiency	22%	38%
Intrinsic $\bar{\nu}_e$ fraction	$10^{-3}$	$10^{-3}$
Intrinsic $\bar{\nu}_e$ norm. unc.	30%	30%

TABLE I. Experimental assumptions used to estimate sensitivity to neutrinophilic forces.

scenario [22], which can be extended to multiple couplings by summing over final states (solid line in Fig. 3). A similar but model-dependent constraint, assuming coupling of the new  $\phi$  field to the Higgs and the lepton doublets at dimension 6, can also be derived [22] from the invisible Higgs width (dashed line in Fig. 3). Sub-leading constraints from cosmology, Supernova 1987A, double beta decay, and  $D$  meson decays are collected in Ref. [22], and found to be much weaker than the invisible  $Z$  width constraints in the space of interest.

### EXPLORATION WITH FUTURE MUON DECAY-AT-REST PROGRAMS

Neutrino experiments using non-DAR sources are dominated by processes with only one neutrino per decay (in MiniBooNE [7], for example, sub-% level flux contributions arise from muon decay [27]), and thus this transmutation effect will be unobservable there. However, future DAR programs such as OscSNS [28] and JSNS<sup>2</sup> [29], both conceived to study the LSND anomaly directly, could observe the effect outlined here.

We have estimated the sensitivity of both OscSNS and JSNS<sup>2</sup>, given experimental assumptions shown in Table I [28, 29]. The dominant background to a signal of oscillated or transmuted  $\bar{\nu}_e$  in both OscSNS and JSNS<sup>2</sup> is the intrinsic  $\bar{\nu}_e$  contamination originating from  $\mu^-$  that fails to capture in the target/shielding material, followed by decay ( $\mu^- \rightarrow e^- \bar{\nu}_e \nu_\mu$ ). The background  $\bar{\nu}_e$  energy spectrum is fundamentally different than the signal for both energy-independent transmutations and most combinations of possible neutrino oscillation parameters (see Fig. 4), however. Along with the relevant accelerator/source and detector parameters, this intrinsic  $\bar{\nu}_e$  fraction and uncertainty ( $10^{-3}$  and 30%, respectively, for both experiments) are crucially important. Fig. 4 shows example JSNS<sup>2</sup> spectra for the transmuted signal and  $\bar{\nu}_e$  background, given a 5 calendar year exposure and an example oscillated signal parameter set ( $\Gamma = 4$ ,  $g_1 = 0.3$ ,  $g_2 = 0.2$ ,  $g_3 = 0.1$ ). The sensitivities of JSNS<sup>2</sup> and OscSNS, determined using a profile log-likelihood

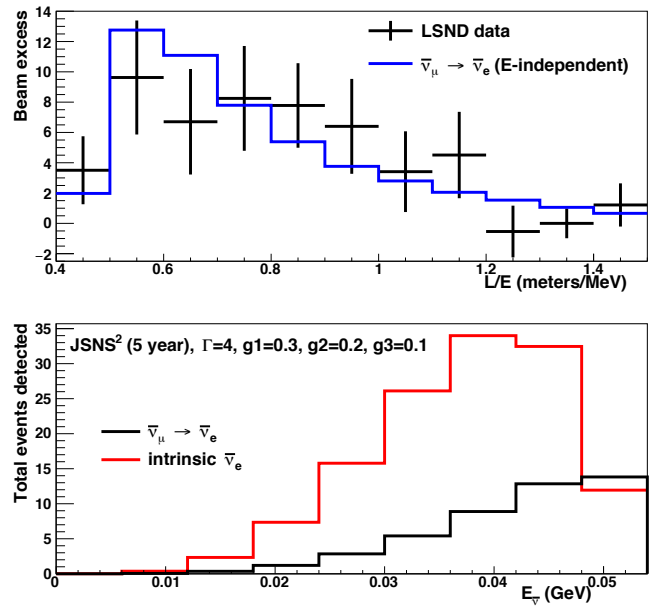


FIG. 4. (Top) The LSND beam excess overlaid on the distribution expected for energy-independent transmutations. (Bottom) Example transmuted signal and background spectra for JSNS<sup>2</sup>, given a 5 calendar year exposure and the neutrinophilic force parameters specified.

technique [30] treating the intrinsic  $\bar{\nu}_e$  background as a nuisance parameter, are shown in Fig. 5 for two example sets of parameters. The LSND allowed region would be entirely excluded by both programs at more than 90% CL in both cases. This conclusion is maintained at all values of  $g_1$  and  $\Gamma$  explored in the range  $0.5 < \Gamma < 5$  and  $0 < g_1 < 0.5$ . Thus, both JSNS<sup>2</sup> and OscSNS would provide a definitive statement about this particular interpretation of the LSND anomaly.

### CONCLUSIONS

We have re-examined a frequently considered beyond-standard-model scenario in which a neutrino portal connects neutrinos to new secret interactions mediated by massive particles below the weak scale. The implied short-range forces between neutrinos would generate new flavor-changing phases for neutrinos and antineutrinos in close proximity. If this force is non-mass-universal, the emerging neutrino-antineutrino pair in muon decay would produce partially flavor-transformed states. For mediators in the mass range between the kaon mass and the  $W$  mass,  $O(0.1)$  couplings are weakly constrained experimentally. With couplings of this scale, there is a significant available parameter space that can produce flavor changes consistent with the LSND anomaly. Tensions with other experimental neutrino programs based on pion or nuclear decay are effectively ameliorated, and future experiments such as JSNS<sup>2</sup> or OscSNS will be able

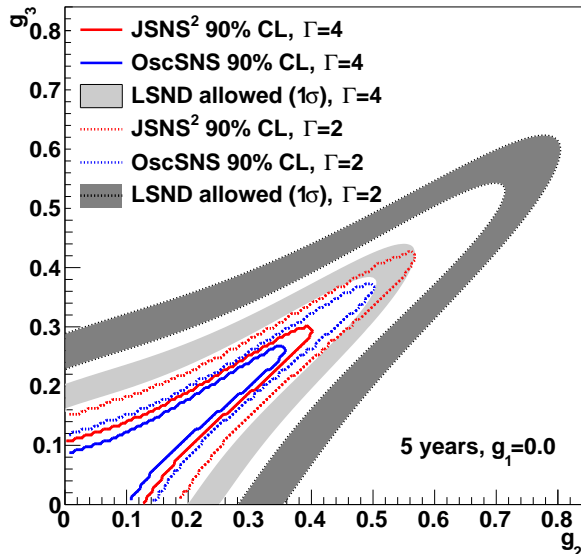


FIG. 5. The sensitivity of JSNS<sup>2</sup> and OscSNS to neutrinophilic forces.

to sensitively explore this possible effect, distinguishing it from signatures of other beyond-standard-model explanations of the LSND anomaly such as sterile neutrinos.

### ACKNOWLEDGEMENTS

We thank Carlos Argüelles, André De Gouvea, Johnathon Jordan, Yoni Kahn, Gordan Krnjaic, Bill Louis, and Pedro Machado for fruitful discussion about this work and their comments on the manuscript. BJPJ acknowledges the support of the Department of Energy under Early Career Award DE-SC0019054. JS is supported by the Department of Energy, Office of Science, under Award No. DE-SC0007859.

---

[1] C. Athanassopoulos et al. The Liquid Scintillator Neutrino Detector and LAMPF Neutrino Source. *Nucl. Instrum. Meth.*, A388:149–172, 1997.

[2] A. Aguilar-Arevalo et al. Evidence for Neutrino Oscillations from the Observation of Anti-neutrino(electron) Appearance in a Anti-neutrino(muon) Beam. *Phys. Rev.*, D64:112007, 2001.

[3] K.N. Abazajian et al. Light Sterile Neutrinos: a White Paper. *arXiv:1204.5379*.

[4] R.L. Burman, M.E. Potter, and E.S. Smith. Monte Carlo Simulation of Neutrino Production by Medium-energy Protons in a Beam Stop. *Nucl. Instrum. Meth. A*, 291(3):621–633, 1990.

[5] G.H. Collin, C.A. Argüelles, J.M. Conrad, and M.H. Shaevitz. Sterile Neutrino Fits to Short Baseline Data. *Nucl. Phys.*, B908:354–365, 2016.

[6] M. Maltoni. Sterile Neutrinos - the Global Picture, June 2018. [Presentation at Neutrino2018]: <https://doi.org/10.5281/zenodo.1287015>.

[7] A.A. Aguilar-Arevalo et al. Significant Excess of Electron-Like Events in the MiniBooNE Short-Baseline Neutrino Experiment. *Phys. Rev. Lett.*, 121(22):221801, 2018.

[8] M.G. Aartsen et al. Searches for Sterile Neutrinos with the IceCube Detector. *Phys. Rev. Lett.*, 117(7):071801, 2016.

[9] P. Adamson et al. Search for Sterile Neutrinos in MINOS and MINOS+ using a Two-detector Fit. *Phys. Rev. Lett.*, 122(9):091803, 2019.

[10] K.C.Y. Ng and J.F. Beacom. Cosmic Neutrino Cascades from Secret Neutrino Interactions. *Phys. Rev.*, D90(6):065035, 2014. [Erratum: *Phys. Rev.* D90(8):089904, 2014].

[11] P. Bakhti, Y. Farzan, and M. Rajaei. Secret interactions of neutrinos with light gauge boson at the DUNE near detector. *Phys. Rev.*, D99(5):055019, 2019.

[12] J. Asaadi, E. Church, R. Guenette, B.J.P. Jones, and A.M. Szelc. New Light Higgs Boson and Short-baseline Neutrino Anomalies. *Phys. Rev.*, D97(7):075021, 2018.

[13] P.A.N. Machado, Y.F. Perez, O. Sumensari, Z. Tabrizi, and R.Z. Funchal. On the Viability of Minimal Neutrinophilic Two-Higgs-Doublet Models. *JHEP*, 12:160, 2015.

[14] E. Bertuzzo, P.A.N. Machado, Z. Tabrizi, and R.Z. Zukanovich. A Neutrinophilic 2HDM as a UV Completion for the Inverse Seesaw Mechanism. *JHEP*, 11:004, 2017.

[15] K. Huitu, T.J. Karkkainen, S. Mondal, and S.K. Rai. Exploring Collider Aspects of a Neutrinophilic Higgs Doublet Model in Multilepton Channels. *Phys. Rev.*, D97(3):035026, 2018.

[16] S. P. Mikheyev and A. Yu. Smirnov. Resonance Amplification of Oscillations in Matter and Spectroscopy of Solar Neutrinos. *Sov. J. Nucl. Phys.*, 42:913–917, 1985.

[17] L. Wolfenstein. Neutrino Oscillations in Matter. *Phys. Rev.*, D17:2369–2374, 1978.

[18] R.M. Crocker, C. Giunti, and D.J. Mortlock. Neutrino Interferometry in Curved Space-time. *Phys. Rev.*, D69:063008, 2004.

[19] N. Fornengo, C. Giunti, C.W. Kim, and J. Song. Gravitational Effects on the Neutrino Oscillation. *Phys. Rev.*, D56:1895–1902, 1997.

[20] H. Yukawa. On the Interaction of Elementary Particles I. *Proc. Phys. Math. Soc. Jap.*, 17:48–57, 1935. [Prog. Theor. Phys. Suppl.1,1(1935)].

[21] M. Tanabashi et al. Review of Particle Physics. *Phys. Rev. D*, 98(3):030001, 2018.

[22] J.M. Berryman, A. de Gouvea, K.J. Kelly, and Y. Zhang. Lepton-Number-Charged Scalars and Neutrino Beamstrahlung. *Phys. Rev.*, D97(7):075030, 2018.

[23] K. Eitel et al. The Search for Neutrino Oscillations Muon Anti-neutrino to Electron Anti-neutrino with KARMEN. *Proceedings, International Conference on Neutrino Physics and Astrophysics (Neutrino'98): Takayama, Japan, June 4-9, 1998*.

[24] G.J. Feldman and R.D. Cousins. A Unified Approach to the Classical Statistical Analysis of Small Signals. *Phys. Rev.*, D57:3873–3889, 1998.

- [25] A.P. Lessa and O.L.G. Peres. Revising Limits on Neutrino-Majoron Couplings. *Phys. Rev.*, D75:094001, 2007.
- [26] ALEPH, DELPHI, L3, OPAL, and SLD Collaborations, LEP Electroweak Working Group, SLD Electroweak Group, and SLD Heavy Flavour Group. *Phys. Reports*, 427(257), 2006.
- [27] A.A. Aguilar-Arevalo et al. The Neutrino Flux Prediction at MiniBooNE. *Phys. Rev.*, D79:072002, 2009.
- [28] M. Elnimr et al. The OscSNS White Paper. In *Proceedings, 2013 Community Summer Study on the Future of U.S. Particle Physics: Snowmass on the Mississippi (CSS2013): Minneapolis, MN, USA, July 29-August 6, 2013*.
- [29] S. Ajimura et al. Technical Design Report (TDR): Searching for a Sterile Neutrino at J-PARC MLF (E56, JSNS2). 2017.
- [30] W.A. Rolke, A.M. Lopez, and J. Conrad. Limits and Confidence Intervals in the Presence of Nuisance Parameters. *Nucl. Instrum. Meth.*, A551:493–503, 2005.
- [31] F. Halzen and A.D. Martin. *Quarks and Leptons: An Introductory Course in Modern Particle Physics*. 1984.
- [32] M. Thomson. *Modern Particle Physics*. Cambridge University Press, 2013.

## APPENDIX: INITIAL SEPARATION OF NEUTRINOS IN MUON DECAY

In this Appendix, we quantitatively motivate that the initial separation of the two neutrinos emerging from muon decay is  $O(1/m_W)$ , rather than the alternative distance scale in the problem  $O(1/m_\mu)$ . The amplitudes for particle decays in quantum field theory are traditionally calculated via the Feynman expansion. The results are scattering amplitudes from momentum eigenstates in the infinite past to momentum eigenstates in the infinite future, erasing all information about positions and times of interactions in between. This is usually appropriate, since such intermediate state information is unobservable in, for example, decay lifetime or scattering cross section calculations. However, it makes the Feynman expansion an imperfect tool for addressing the question at hand.

Feynman diagrams for elastic scattering are often motivated in textbooks (e.g. Refs. [31, 32]) by comparison to potential scattering with one particle at rest. It is shown that, for example, the scattering of two particles via a massless mediator is equivalent to the scattering of one particle from another as the source of a Coulomb potential. The former approach has the advantage of making Lorentz invariance explicit while hiding position-space information, whereas the latter makes the position-space description explicit while obscuring Lorentz invariance. Here we will reverse the usual argument, introducing a flavor-changing potential  $V$  for muon decay, by analogy to the case of elastic scattering. We will ignore spin and its consequences, since we are only concerned with establishing the distance scale of the propagator.

The flavor-changing potential  $V$  includes the creation

and annihilation operators to destroy muons and create the final state particles. We enforce that these operations are local, in the sense that particles emerging from a common vertex must have been annihilated/created at the same position in space. However, the mediator has a range, encoded in a function  $f(\vec{r})$ . Thus:

$$V = \int d^3\vec{r} d^3\vec{y} f(\vec{r}) (a_\mu^\dagger(\vec{y}) a_\nu(\vec{y}) a_{\bar{\nu}}(\vec{y} - \vec{r}) a_e(\vec{y} - \vec{r}) + h.c.). \quad (11)$$

To match the usual Feynman diagram calculation, we would specify in- and out-going states to be plane waves:

$$|\mu\rangle = \int dx e^{ip_\mu x_\mu} |\mu(x_\mu)\rangle \dots \quad (12)$$

and so on. Substituting these into Eq. 11 we can obtain:

$$= \int d^3y d^3r f(\vec{r}) e^{i(p_\mu y - p_e(y-r) - p_\nu y - p_{\bar{\nu}}(y-r))}. \quad (13)$$

Integrating over  $\vec{y}$  gives us a momentum conserving delta function, leaving only the integral over interaction range  $\vec{r} = \vec{x}_\mu - \vec{x}_e$ :

$$= \delta(\vec{p}_\mu - \vec{p}_\nu - \vec{p}_e - \vec{p}_{\bar{\nu}}) \int d^3\vec{r} f(\vec{r}) e^{i\vec{q}\vec{r}}, \quad (14)$$

where  $\vec{q} = \vec{p}_e - \vec{p}_{\bar{\nu}}$  is the momentum transfer. The question then, is what choice of  $f(\vec{r})$  will give us the Feynman propagator for an intermediate particle of mass  $m_W$ ? The answer is the Yukawa form:

$$f = V_{Yukawa}(r) = g_a g_b \frac{1}{r} e^{-m_W r}. \quad (15)$$

Which can be easily verified by substitution. Indeed, Yukawa motivated his potential through very similar arguments regarding the range of the nuclear force. Constructing the problem in this “old-fashioned” way allows us to explicitly ask questions about spatial properties of the production state. For example, in this construction we may ask, what is the probability of producing the electron a distance  $\vec{r}'$  away from the muon? The relevant amplitude would be:

$$\langle \mu(\vec{x}_\mu) | V | \nu(\vec{x}_\mu) \bar{\nu}(\vec{x}_\mu + \vec{r}') e(\vec{x}_\mu + \vec{r}') \rangle = f(\vec{r}'), \quad (16)$$

and the probability is the square of this amplitude. To find the mean range we need to calculate the expectation of the  $\hat{r}$  operator, given a suitably normalized probability distribution, which can be expressed as:

$$\langle r \rangle = \frac{\int dr r |f(r)|^2}{\int dr |f(r)|^2} = \frac{2m_W}{4m_W^2} = \frac{1}{2m_W}. \quad (17)$$

We thus conclude that the expected separation at production is related to the mediator mass by  $\langle r \rangle \sim 1/2m_W$ .